Phonon and photon correlation functions for a continuously driven system evolved through the hierarchical equations of motion

Ben S. Humphries,[1] Dale Green,[1] Magnus O. Borgh,[2] and Garth A. Jones[1]

1) School of Chemistry, University of East Anglia, Norwich Research Park, Norwich, NR4 7TJ, UK

2) Physics, Faculty of Science, University of East Anglia, Norwich Research Park, NR4 7TJ, UK

Email: *b.humphries@uea.ac.uk*

Deriving Hierarchical Equations of Motion

1 We define a full molecular system, in stages of increasing complexity, starting with the electronic energy and associated coherences. This forms the system Hamiltonian of our OQS.

2 Molecules in the system of interest are free to interact with other particles, termed the environment/bath, as they would in experiments. This is described mathematically as a coupling H_{SB}.

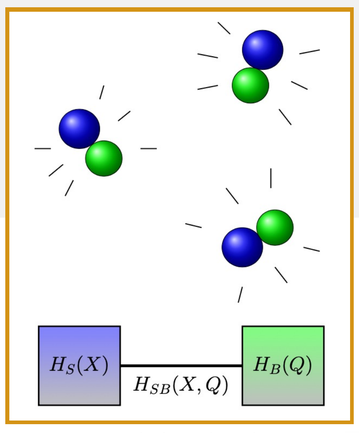

Fig 1: System-bath coupling schematic.

3 This system is then evolved through time in density matrix form. Further interactions are defined through introduction of the Lagrangian.

$$\hat{\rho}_t(q,\mathbf{x}) = \exp\left(\frac{i\hat{H}(q,\mathbf{x})t}{\hbar}\right)\hat{\rho}_0(q,\mathbf{x})\exp\left(\frac{-i\hat{H}(q,\mathbf{x})t}{\hbar}\right).$$

Path integration splits the Lagrangians into exponentials of actions,[2] corresponding to the influence of each component of the OQS on the classical trajectory. The memory of past states, through the infinite paths, are introduced but not resolved fully within the influence functional $\mathcal{F}$.

$$\rho_t(q_t,q_t') = \iint_{q_0}^{q_t}\int_{q_0'}^{q_t'}\rho_0(q_0,q_0')\exp(iS_S[q(\tau);t]/\hbar)\mathcal{F}\exp(-iS_S[q'(\tau);t]/\hbar)\mathcal{D}[q'(\tau)]\mathcal{D}[q(\tau)]\mathrm{d}q_0'\mathrm{d}q_0$$

$$\mathcal{F}[q(\tau),q'(\tau)] = \iiiint\rho_0(\mathbf{x}_0,\mathbf{x}_0')exp\Big[\frac{i}{\hbar}(S_B[(x)(\tau);t]-S_B[(x)'(\tau);t])+ S_{SB}[q(\tau),\mathbf{x}(\tau);t]-S_{SB}[q'(\tau),\mathbf{x}'(\tau);t]\Big]\mathcal{D}[\mathbf{x}'(t)]\mathcal{D}[\mathbf{x}(t)]\mathrm{d}\mathbf{x}_0'\mathrm{d}\mathbf{x}_0$$

4 Take the influence functional and solve the constituent Euler-Lagrange equation of motion with a Green's function to find the influence kernels, iL_1 and L_2.

$$L(t) = L^{(1)}(t) + L^{(2)}(t),$$

$$L^{(1)}+L^{(2)} = \frac{1}{\pi}\int_0^\infty 2\lambda\gamma\frac{\omega\gamma}{\gamma^2+\omega^2}\coth\left(\frac{\beta\hbar\omega}{2}\right)\cos(\omega t)\,\mathrm{d}\omega - \frac{i}{\pi}\int_0^\infty 2\lambda\gamma\frac{\omega\gamma}{\gamma^2+\omega^2}\sin(\omega t)\,\mathrm{d}\omega.$$

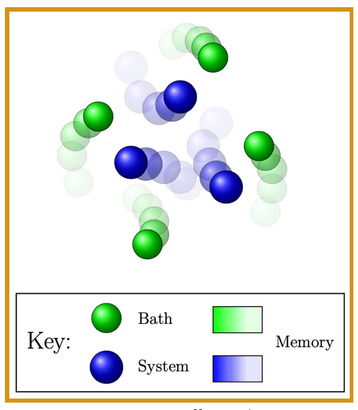

Fig 2: Memory effects schematic.

We finally resolve individual memory components through a Matsubara decomposition, or contour integral.

$$\mathcal{F}(\alpha,\alpha':t) = \exp\left(-\sum_l\int_0^t\hat{V}_l^X(\alpha,\alpha';t)\times\left[\frac{\partial}{\partial\tau}\int_0^\tau i\bar{L}_{1,l}(\tau-\tau')\hat{V}_l^o(\alpha,\alpha';t)\mathrm{d}\tau'+\int_0^\tau L_{2,l}(\tau-\tau')\hat{V}_l^X(\alpha,\alpha';t)\mathrm{d}\tau\mathrm{d}\tau'\right]\right)$$

5

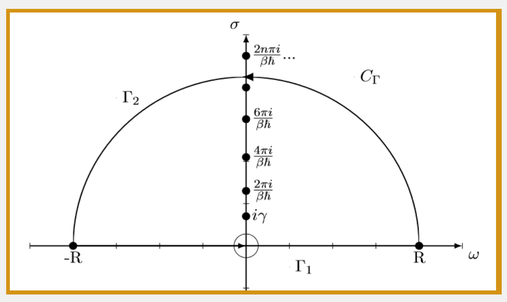

Fig 4: A complex contour in frequency space used to solve the correlation function. Residues of the poles correspond to Matsubara frequencies.

$$\hat{\rho}_n(\alpha,\alpha',t) = \exp(iS[\alpha])\mathcal{F}(\alpha,\alpha';t)\exp(-iS[\alpha'])\times\prod_l\prod_k\left[\int_0^t\exp(-\gamma_k(t-\tau'))\hat{\theta}_{lk}(\alpha,\alpha',t)+\hat{\Gamma}_{lk}(\alpha,\alpha',t)\right]^{n_{lk}}$$

An equation for the ADOs is obtained, but to produce an equation of motion for the density matrix we must be able to traverse the hierarchy structure. Successively apply the chain rule and product rule to achieve 'raising' and 'lowering' terms.

- Why do this?

Solutions to the system of equations are stationary points of the action functional.

- How does it work?

An ODE is solved for a single point - $\boldsymbol{\delta}_s$. Superposition then creates the full solution.

6

$$\dot{\rho}_{\mathbf{j}}(t) = -\left(\mathcal{L}+\sum_{k=0}^{M}j_k\nu_k-\sum_{k=M}^{\infty}\hat{V}_S^\times\hat{\Psi}_k\right)\rho_{\mathbf{j}}(t)+\sum_{k=0}^{M}\hat{V}_S^\times\rho_{j_k^+}(t)+ j_0\hat{\Theta}^-\rho_{j_0^-}(t)+j_1\hat{\Theta}^+\rho_{j_1^-}(t)+\sum_{k=2}^{M}j_k\nu_k\hat{\Psi}_k\rho_{j_k^-}(t),$$

$$\hat{\Psi}_k = \frac{4\eta}{\hbar\beta}\frac{\gamma\omega_0^2}{(\omega_0^2+\nu_k^2)^2-\gamma^2\nu_k^2}\hat{V}_S^\times,$$

$$\hat{\Theta}^\pm = \frac{\eta\omega_0^2}{2\zeta}\left\{\mp\hat{V}_S^\circ\pm\coth\left(\frac{\hbar\beta}{2}\left(\mp\zeta+i\frac{\gamma}{2}\right)\right)\hat{V}_S^\times\right\}$$

Termination[5] upon reaching convergence parameter, ξ, at assumed Markovian limit $\quad\frac{2(M+1)\pi}{\hbar\beta}>\xi,\ \sum_{k=0}^{M}j_k|\mathbf{Re}(\nu_k)|>\xi.$

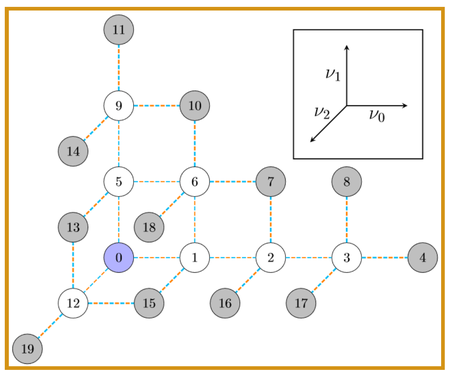

Fig 5: An hierarchy diagram for the HEOM showing connections between ADOs. Grey nodes are termination ADOs, cyan lines move towards the density matrix, orange move away.

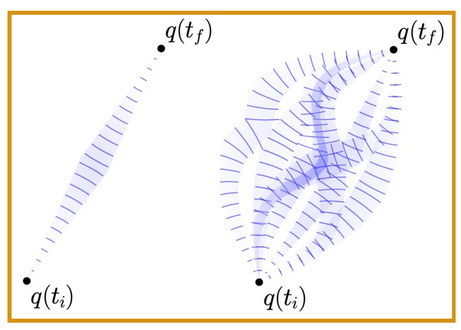

Fig 3: Schematic of a path integral. Left is a single trajectory, right the summation of many which – like a phase – produce a dominant contribution.

Spectral Densities

The bath is defined[1] as a linear combination of delta functions corresponding to an ensemble of environment modes. The profile is taken as a continuous spectral density function.

$$J(\omega) = \sum_\alpha\frac{g_\alpha^2}{2m_\alpha\omega_\alpha}\delta(\omega-\omega_\alpha)$$

Different hierarchical equations of motion can be derived by inputting different forms of function.

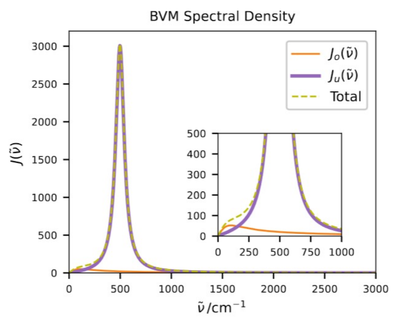

Fig 6: Showing the underdamped spectral density based on work by Fujihashi et al[3] and how its components are subsumed. The orange, as in the flow charts, is overdamped, yellow underdamped, and purple the intramolecular vibration.

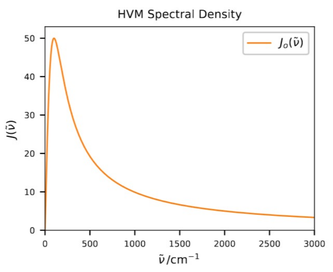

Fig 7: The equivalent overdamped spectral density. It is a redshifted Gaussian profile for an ensemble of delta functions.

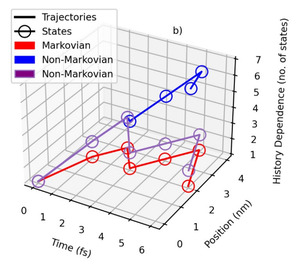

Different spectral densities impart different magnitudes of non-Markovianity to their HEOMs, relative to the damping strength.

Fig 8: Depicting Markovianity, showing state history dependence in 3D.

Two-time Correlation Functions

In order to better understand non-classical, coherence behaviours we apply statistical correlation functions. From the scattered light field we can produce two orders of two time correlation function.

$$\hat{\mathbf{E}}^+ = \frac{a^\dagger(t)\exp(i\mathbf{k}\cdot\mathbf{r})}{\epsilon_0}$$

$$g^{(1)}(\tau) = \langle\hat{\mathbf{E}}^-(t)\hat{\mathbf{E}}^+(t+\tau)\rangle,$$

$$g^{(2)}(\tau) = \langle\hat{\mathbf{E}}^-(t)\hat{\mathbf{E}}^-(t+\tau)\hat{\mathbf{E}}^+(t+\tau)\hat{\mathbf{E}}^+(t)\rangle$$

$$g_C^{(1)}(t,\tau) = \frac{\mathbf{Tr}\left[C\exp(\mathcal{L}\tau)(\rho C^\dagger)\right]}{\mathbf{Tr}(C\rho C^\dagger)},$$

$$g_C^{(2)}(t,\tau) = \frac{\mathbf{Tr}\left[C^\dagger C\exp(\mathcal{L}\tau)(C\rho C^\dagger)\right]}{\mathbf{Tr}(C\rho C^\dagger)^2}.$$

$$g_{CD}^{(2)}(t,\tau) = \frac{\mathbf{Tr}\left[C^\dagger C\exp(\mathcal{L}\tau)(D\rho D^\dagger)\right]}{\mathbf{Tr}(C\rho C^\dagger)\mathbf{Tr}(D\rho D^\dagger)}$$

Expectation values of two-time products of operators cannot be simply computed, but can be reformulated using the Quantum Regression formula of Lax et al.[4]

For an arbitrary operator, C, (where here we use creation and annihilation of photons 'a' and phonons 'b') the reformulated orders of correlation function are shown.

If D is an equivalent arbitrary operator then we can produce a cross-correlation[6,7] for multiple particle types. These equations[8] are used in conjunction with HEOM dynamics along times t and **τ** ps.

A model monomer system:

$$h_g = \hbar\omega_0\left(b^\dagger b+\tfrac{1}{2}\right),$$

$$h_e = \hbar(\omega_{eg}^0+\lambda)+\hbar\omega_0\left(b^\dagger b-\frac{\Delta}{\sqrt{2}}(b+b^\dagger)+\tfrac{1}{2}\right)$$

$$\mathrm{H}_{SB} = \frac{p^2}{2m}+\frac{1}{2}m\omega_0^2\left(x-\frac{gB^2}{2m\omega_0^2}\right)$$

$$\mathrm{H}_{SF} = \mu\exp\left(\frac{i\omega_{eg}^0}{\hbar}\right)+\mu^*\exp\left(\frac{-i\omega_{eg}^0}{\hbar}\right)$$

A simple molecular system is chosen as a test case. A two level system, where the excited state can be displaced. This is evolved through the HEOM and, after initialisation, a continuous field drives the system.

We run a series of models for different values of the bath and system reorganisation energies **η** and **λ**.

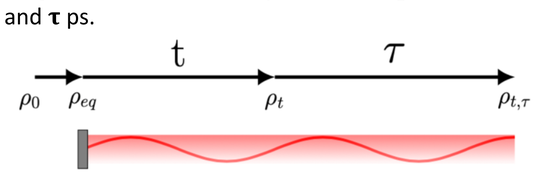

Fig 9: Schematic showing evolution time, states of the density matrix, and the continuous driving field.

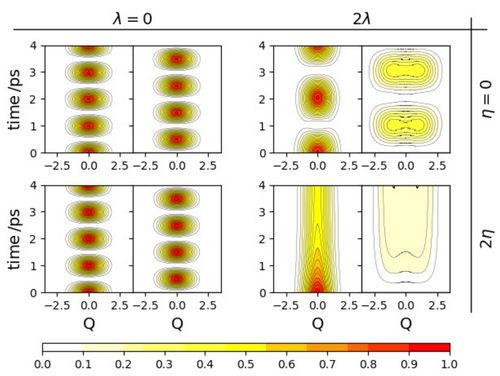

Fig 10: Wavepacket evolution for four different values of system and bath reorganisation energy.

Results: Correlation Functions of a Monomer

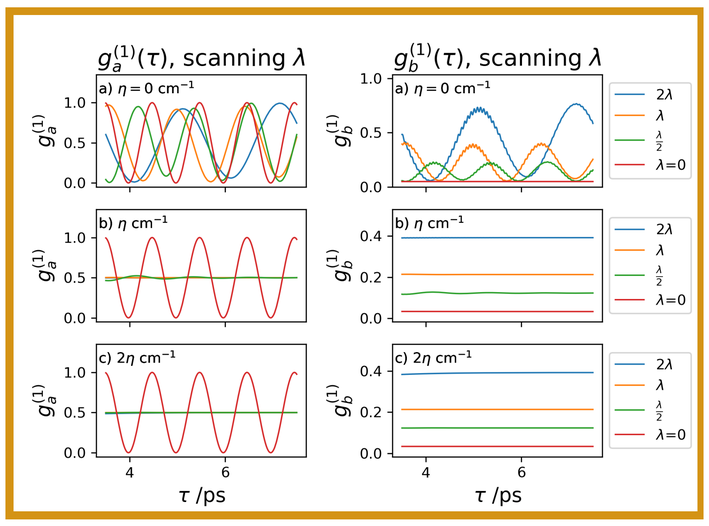

Fig 11: First order two-time correlation functions for photons and phonons

- First Order

The $g_a^{(1)}$ tracks the population of the excited state when there is no bath. As bath reorganisation energy increases the rabi oscillations are damped more strongly. $g_b^{(1)}$ is constant in the steady state and without bath influence and increases linearly with system excited state displacement.

- Second Order

$g_a^{(2)}$ amplitudes are dependent on $g_a^{(1)}$ and, with the exception of **η**=0, increase in damping with **λ**. $g_a^{(2)}$ follows the same trend as its first order counterpart, but mode frequency is more evident. The cross correlation functions have the behaviour of the initial mode superimposed on the latter.

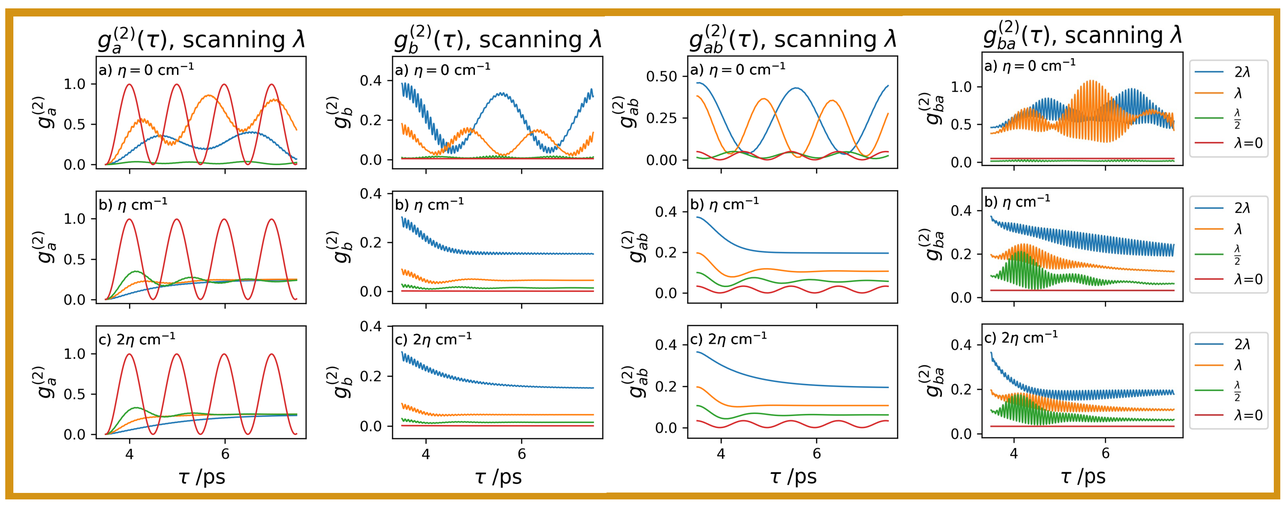

Fig 12: Second order two-time correlation functions for photons and phonons, and the two forms of the cross-correlation function.

Summary

Many types of HEOM can be derived from different spectral densities in order to have fine control over the damping and memory effects. Additionally, photons and phonons appear to be significantly influenced by the presence of an external bath. Finally, the cross-correlation functions show considerable possibility for bunching and anti-bunching of photons and phonons. This research was carried out on the ADA Cluster supported by the Research and Specialist Computing Support service at UEA.

Future Research

- Next we intend to finish development of a full derivation of our own HEOM method.
- How two-time correlation functions are impacted by increasing non-Markovianity.
- Study of virtual information transfer within the hierarchy structure.

References

1. D. Green, B. S. Humphries, A. G. Dijkstra, and G. A. Jones, J. Chem. Phys. 151, 1 (2019).
2. Y. Tanimura, Phys. Rev. A 41, 6676 (1990).
3. Y. Fujihashi, G. R. Fleming, and A. Ishizaki, J. Chem. Phys. 142(2015), 10.1063/1.4914302, arXiv:1505.05281.
4. M. Lax, Phys. Rev. 129, 2342 (1963).
5. A. G. Dijkstra and V. I. Prokhorenko, J. Chem. Phys. 147, 1 (2017)
6. M. Moslehi, H. R. Baghshahi, M. J. Faghihi, and S. Y. Mirafzali, Eur. Phys. J. Plus 137, 777 (2022).
7. T.-t. Ma, D. B. Horoshko, C.-s. Yu, and S. Y. Kilin, Phys. Rev. A 105, 1 (2022), arXiv:2205.01312.
8. H. J. Carmichael and D. F. Walls, J. Phys. B At. Mol. Phys. 9, 1199 (1976).